

## **DISPLACEMENT FIELD GRADIENT MEASUREMENT USING THE SPECKLE PHOTOGRAPHY METHOD**

**JERZY TADEUSZ PISAREK**

*Institute of Mechanics and Machine Design Foundations  
Technical University of Częstochowa*

Discussion of the effect of relative displacements gradient on the Fourier halo of specklegram has been conducted. It was predicted theoretically that the energy distribution of the Fourier halo obtained from the point-by-point analysis of a specklegram depends both on the type of basic speckle structure, and the Fourier transform of a diaphragm shape function for the optical Fourier processor applied. Scale factors of this transform are linear combinations of gradient tensor components. A type of the speckle structure is determined by the characteristic function, defined as a sum of double convolution of the speckle shape function. The theoretical results were verified experimentally for various configurations of translation, strain and rotation, respectively.

### **1. Introduction**

Speckle photography is the optical method for displacement measurement. At the first step of measurement process a double exposure photography (before and after a movement) of the stochastic speckle pattern is registered. The resulting transparency, called a specklegram after photo-chemical developing is analyzed in the whole field or point by point, using the Fourier optical processors. Depending on the kind of relation between the speckle pattern and the tested object motions, respectively, and taking the way of speckle generating into account, many techniques of speckle photography can be specified. Initially, the speckle photography was used only in determination of those rigid body surface translation components, which were perpendicular to the line of sight (cf Archbold et al. (1970)). Chiang and Juang (1976a,b) applied this method to determination of static or dynamic angular displacements. The basic speckle pattern was obtained due to the laser beam scattered on a rough

surface interference. Forno (1975) made a speckle pattern of very fine granularity in spatial coherent white light. The object surface, before illuminating, was coated with a special spatial reflective paint. Forno (1975) proposed the measurement technique which he called "white light speckle photography", however, according to the current nomenclature it should be called "white light interferometry" or "shearing interferometry". White light specklegrams were for the first time obtained by Chiang and Bailangadi (1980) and Bachmacz and Pisarek (1980), (1983), using the method in which the speckle pattern was projected onto the object surface treated as a screen. The speckle projection method enabled determination of the object surface displacement components, which were perpendicular to the surface. In his Ph. D. dissertation, Pisarek (1986) used a very simple method for generating the speckle pattern. On the black object surface an aluminium powder was sputtered. White light speckle patterns of high contrast were observed illuminated by a typical reflector. White light methods extended the range and ratio of speckle photography and made it possible to be applied under polygon conditions. In the same dissertation a light knife technique application to 3D gas flow measurement was proposed. Iwata et al. (1978) applied the speckle photography to 2D fluid flow investigation. A very thorough and detailed description of this method supplied with a computer speckle analysis was presented by Dudderar (1988). In 1984 J.Lira applied white light speckle photography to determination of the density distribution in a flowing transparent medium.

The speckle photography techniques given above prove widespread practical application of the method, specially to strain measurement. The measurement is non-contact, cheap and more accurate then the conventional strain gauge method. The speckle photography can be useful in testing important elements, which should be supervised, since the specklegram obtained is the source document which practically cannot be falsified.

Unfortunately, rapid development of the specklegram recording techniques does not involve the specklegram analysis methods advance. The description of specklegram halo used nowadays still follows the procedure formulated by Tokarski and Burch (1968), who discussed only the simplest displacement state, i.e. pure translation. Parks (1980) presented the experimental results proving the influence of rotation and strain on the fringe pattern contrast. He did not propose, however, a mathematical model for quantitative description of the observed effect. In 1984 Pisarek gave the lecture at the XIII Conference on Mathematic Application, in which he presented the theorem of relative displacement coefficient. The proof and applications of this theorem have not been published yet. At the GAMM'94 conference the author presented the concept of characteristic function application to a quantitative description of

almost all kinds of the speckle pattern. In author's opinion, application of these theoretical results to a numerical analysis of specklegram Fourier halos must result in small measurement errors.

## 2. The principle of speckle photography

The basic idea of speckle photography consists in double or multi-exposure registration of the speckle pattern on the same photo plate and analyzing the diffraction halo (Young fringes) or the Fourier halo of final transparency. An example of typical realization of this idea is presented in Fig.1.

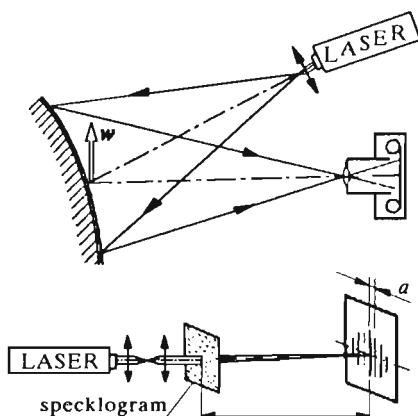


Fig. 1. The idea of registration and the point-by-point analysis of the specklegram

The speckle pattern is generated by means of the He-Ne laser beam scattered on a rough object surface interference. The speckle image is in this case strongly affected by the analyzed surface. Of course, it is only one of the possibilities of speckle pattern generation and one of the ways of the correspondence between the speckle motion and the analyzed object motion establishing, respectively. Another examples of the speckle method are presented in Section 1. The specklegram is recorded on a 10E75 film using a typical camera. It is analyzed point-by-point (Fig.2) in a 2D Fourier optical processor. The Fourier transformation is realized by the system of lens 1. The Fourier halo of the analyzed specklegram region 2 is observed on the focusing screen 3. The resulting fringe pattern can be measured manually, directly on the screen. Using a CCD camera and the computer image processing seems to be more effective.

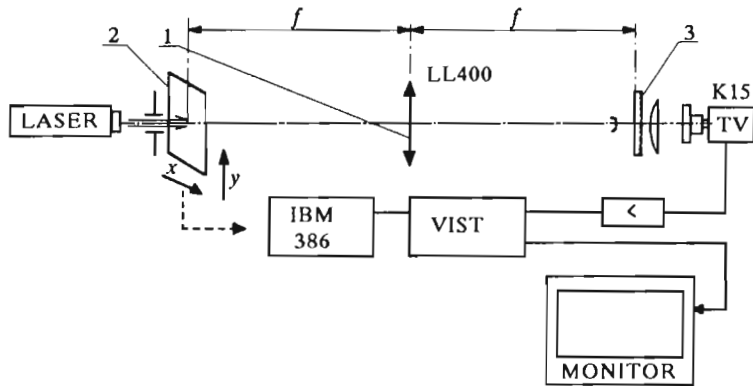


Fig. 2. Optical Fourier processor used in experiments

The condenser placed between the CCD camera objective and the focusing screen focuses the light scattered on the screen in the objective diaphragm. The signal from the CCD matrix is, passing the frame grabber system, transmitted to an IBM personal computer.

The analog part of the processor realizes the transformation

$$A(u, v) = \iint_{-\infty}^{\infty} A_0 K(x, y) t(x, y) \exp\left[\frac{2\pi i}{\lambda f}(ux + vy)\right] dx dy \quad (2.1)$$

where

- $A(u, v)$  – distribution of a complex amplitude of the wave on the Fourier plane (on the focusing screen surface)
- $A_0$  – complex amplitude of the laser beam in the specklegram plane
- $K(x, y)$  – shape function of the analyzed region of the specklegram
- $t(x, y)$  – distribution of optical density of the specklegram
- $x, y$  – coordinates in the specklegram plane (original plane)
- $u, v$  – coordinates in the Fourier plane (on the focusing screen surface).

If two identical images are recorded on the specklegram, shifted by the vector  $\mathbf{w} = [w_x, w_y]$  then its transmittance can be described as follows

$$t(x, y) = t_0(x, y) \otimes [\delta(x, y) + \delta(x + w_x, y + w_y)] \quad (2.2)$$

where

- $t_0(x, y)$  – distribution of transmittance in conventional one-exposure photography of the basic speckle pattern  
 $\delta(\cdot)$  – Dirac function  
 $\otimes$  – convolution symbol.

Because the transformation described by Eq(2.1) is the Fourier transformation

$$A(u, v) = \mathcal{F}(K(x, y)t(x, y))$$

then it must be

$$A(u, v) = A_0(u, v) \left[ 1 + \exp\left(\frac{2\pi i}{\lambda f}(w_x u + w_y v)\right) \right] \quad (2.3)$$

where

$$A_0(u, v) = \mathcal{F}(K(x, y)t_0(x, y)) \quad (2.4)$$

Distribution of the light intensity in the Fourier plane in the case of homogeneous displacement field is described as follows

$$J(u, v) = A(u, v)A^*(u, v) = J_0(u, v) \left[ 1 + \cos\left(\frac{2\pi i}{\lambda f}(w_x u + w_y v)\right) \right] \quad (2.5)$$

where

$J(u, v)$  – light intensity of one-exposure photography of the speckle pattern,  $J(u, v) = A(u, v)A^*(u, v)$

$A^*(u, v)$  – complex amplitude, conjugate to  $A(u, v)$ .

Eq (2.3) is known (cf Francon and Ostrowski [13]) as the Tokarski and Burch theorem. In this paper the theorem will be adapted to the displacement field of large gradient.

### 3. Theorem of the fringe contrast in specklegram halo

Displacement gradient  $\mathbf{G}$  can be separated as a sum of the rotation  $\mathbf{R}$  and strain  $\mathbf{E}$  tensors, respectively

$$\mathbf{G} = \begin{bmatrix} \frac{\partial w_x}{\partial x} & \frac{\partial w_x}{\partial y} \\ \frac{\partial w_y}{\partial x} & \frac{\partial w_y}{\partial y} \end{bmatrix} = \begin{bmatrix} g_{xx} & g_{yx} \\ g_{xy} & g_{yy} \end{bmatrix} = \mathbf{R} + \mathbf{E} \quad (3.1)$$

Distribution of the displacement  $\mathbf{w}(x, y)$  over a small region  $K(x, y)$  can be approximated by the linear function

$$\begin{aligned}w_x(x, y) &= w_{0x} + (x - x_c) \frac{\partial w_x}{\partial x} + (y - y_c) \frac{\partial w_x}{\partial y} \\w_y(x, y) &= w_{0y} + (x - x_c) \frac{\partial w_y}{\partial x} + (y - y_c) \frac{\partial w_y}{\partial y}\end{aligned}\quad (3.2)$$

where  $\mathbf{w}_0 = [w_{0x}, w_{0y}]$  – mean displacement in the region  $K(x, y)$ .

Complex amplitude distribution in the Fourier plane is then described by the following integral

$$\iint_{-\infty}^{\infty} K(x, y) t_0(x, y) \otimes [\partial(x, y) + \delta(x + w_x(x, y), y + w_y(x, y))] \exp\left[\frac{2\pi i}{\lambda f}(ux + vy)\right] dx dy \quad (3.3)$$

The resulting light intensity distribution can be presented in the form

$$\begin{aligned}J(u, v) &= J_0(u, v) \mathcal{F}[\delta(x, y) + \delta(x + w_x, y + w_y)] = \\&= J_0(u, v) \left\{ 1 + N(u, v) \left[ 1 + \cos\left(\frac{2\pi i}{\lambda f}(w_{0x}u + w_{0y}v)\right) \right] \right\}\end{aligned}\quad (3.4)$$

where

$$N(u, v) = \int \int K(x_s, y_s) \exp \frac{2\pi i}{\lambda f} \left( \begin{bmatrix} g_{xx} & g_{yx} \\ g_{xy} & g_{yy} \end{bmatrix} \begin{bmatrix} x_s \\ y_s \end{bmatrix} \right)^T \begin{bmatrix} u \\ v \end{bmatrix} dx_s dy_s \quad (3.5)$$

$$x_s = x - x_c \quad y_s = y - y_c$$

where  $x_c, y_c$  – coordinates of the  $K(x, y)$  region center.

Let us call  $N(u, v)$  the coefficient of relative displacement. The integral in Eq (3.5) is the Fourier transform of the shape function of the analyzed region. The sum of adequate components of rotation and displacement tensors, respectively, stand for scale factors of the transformation. If all components of these tensors tend to zero then the coefficient of relative displacement will tend to 1 in the analyzed region of specklegram halo. The following contrast  $C$  of fringe pattern can be obtained, which is equal to  $N(u, v)$

$$C \stackrel{\text{df}}{=} \frac{J_{\max} - J_{\min}}{J_{\max} + J_{\min}} = \frac{J(u, v) \left[ (1 + N(u, v)) - (1 - N(u, v)) \right]}{J(u, v) \left[ (1 + N(u, v)) + (1 - N(u, v)) \right]} = N(u, v) \quad (3.6)$$

**Theorem.** The contrast of speckle pattern in the Fourier halo of the specklegram recorded on a photo material of linear characteristic equals the Fourier transform of the diaphragm shape function, scale factors  $s_x$  and  $s_y$  of which, i.e., have the form of the following components of displacement gradient

$$s_x = g_{xx} + g_{xy} \quad s_y = g_{yy} + g_{yx} \quad (3.7)$$

#### 4. Light energy distribution in the Fourier halo of the basic speckle pattern

The amplitude transmittance of one-exposure speckle pattern can be presented as follows

$$t(x, y) = \sum_j h_j(x - x_{cj}, y - y_{cj}) \otimes \delta(x_{cj}, y_{cj}) \quad (4.1)$$

where  $x_{cj}, y_{cj}$  — coordinates of the  $j$ th speckle center.

The energy distribution of the Fourier halo has the form

$$J(u, v) = \sum_j h_j^{\otimes 2} + \sum_{k \neq l} \mathcal{F}(h_k h_l) \exp \left[ \frac{2\pi i}{\lambda f} \left( (x_k - x_l)u + (y_k - y_l)v \right) \right] \quad (4.2)$$

For a great number of speckles the mean value of the second component is practically equal to zero. The mean value of Fourier halo energy distribution is equal to the Fourier transform of a sum of double convolutions of images of certain speckles. For a high contrast of speckle pattern to be achieved the distribution should be equal to a sum of double convolutions of the speckle shape functions.

The function

$$H(x, y) \stackrel{\text{df}}{=} \sum_j K_j^{\otimes 2}(x - x_{cj}, y - y_{cj}) \quad (4.3)$$

is called "characteristic function of the speckle pattern". This function is strongly dependent on the roughness grade of the object surface. Having  $H(\cdot)$  obtained is very important for discussion of the class of  $J_0(u, v)$  approximates.

## 5. Experimental results

### 5.1. Speckle pattern

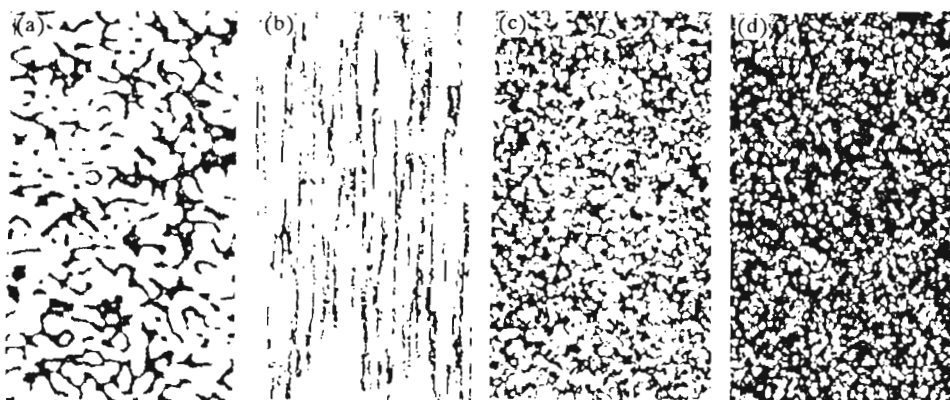


Fig. 3. Images of a typical speckle pattern; (a) – laser speckle on the aluminum surface ( $Ra = 15\mu\text{m}$ ), (b) – laser speckle on the steel surface ( $Ra = 0.3\mu\text{m}$ ), (c) – speckle in white light (Al powder)

A typical speckle pattern generated due to the rough surface is presented in Fig.1. For rough surfaces ( $Ra > 10\mu\text{m}$ ) and great values of numeric aperture of camera objective the pattern (Fig.1a) is homogeneous and practically independent of micro-geometry of the surface. The characteristic function and its Fourier transform are the central symmetrical functions. Light distribution in the Fourier plane of the point-by-point processor can be approximated well by the Gauss function, parameters of which correspond to the aperture of camera objective.

The speckle pattern shape observed on a polished steel surface depends on both the surface roughness and parameters of the illuminating laser beam. The limiting conditions can be formulated in the following form

$$Ra < 2.5 \mu\text{m}$$

$$Sm \gg 1.22\lambda nM$$

where

$Ra$  – mean roughness height

$Sm$  – roughness wave length

$n$  – numerical aperture of the objective

$M$  – camera magnification.



The above conditions have been obtained experimentally in the course of testing a series of steel specimens of different parameters of the surface roughness. For  $Ra < 0.63\mu\text{m}$  the contrast of the speckle pattern is strongly dependent on  $Ra$ . The characteristic function is in this case an axial symmetric one. Light distribution of the Fourier halo of the pattern must be approximated by a multi parameter 2D function.

The speckle pattern obtained in white light (Fig.3c) using the aluminum powder sputtering technology is anisotropic. The characteristic function is a central symmetric one. Light distribution of the pattern Fourier halo can be roughly approximated by the Bessel function with the only parameter  $d$

$$J_0(u, v) = J_0\left(\frac{2\pi d}{\lambda f} \sqrt{u^2 + v^2}\right)$$

where  $J_0$  – cylindrical Bessel function of the first kind.

The parameter  $d$  can be interpreted as the mean speckle diameter in the analyzed pattern. A typical value of  $d$  lies in the range  $d = 10 \div 100\mu\text{m}$ .

## 5.2. Fourier halos for displacements and small strains

Displacement fields in axially tensed strip made of aluminum, plexiglas, titan, CoMoNi alloy (metal glass) and hard rubber, respectively have been recorded on specklegrams. The speckle patterns for all metal specimens were made both in laser beams and in white light. The specimens made of metal glass were tested in laser beam only. Rubber specimens and those made of plexiglas were tested in white light using the powder of about  $100\mu\text{m}$  in diameter. For loading stress values lower then the yield point the resulting specklegram hallos for all the specimens made of rubber and plexiglas can be precisely described by Eq (3.4). For the loading stress exceeding the yield point the contrast of fringes in the specklegram halo has been markedly lower then the value calculated after the theory presented above, which can be explained by local discontinuities of the displacement and strain fields, respectively. When testing specimens made of thin (0.05 mm) metal glass foil (Fig.4) the fringe pattern contrast varied with the distance from the specimen edge, being slightly higher at the specimen edge then the value calculated from Eqs (3.5) and (3.6). In the specimen axis, however it has become very low.

The specklegram halos presented in Fig.4 have been obtained in the course of analysis of the regions situated 1.2 mm from edge of the strip of 10 mm in width. The distance between successive measurement points was 2 mm. The histograms of light distribution have been obtained in the region localized

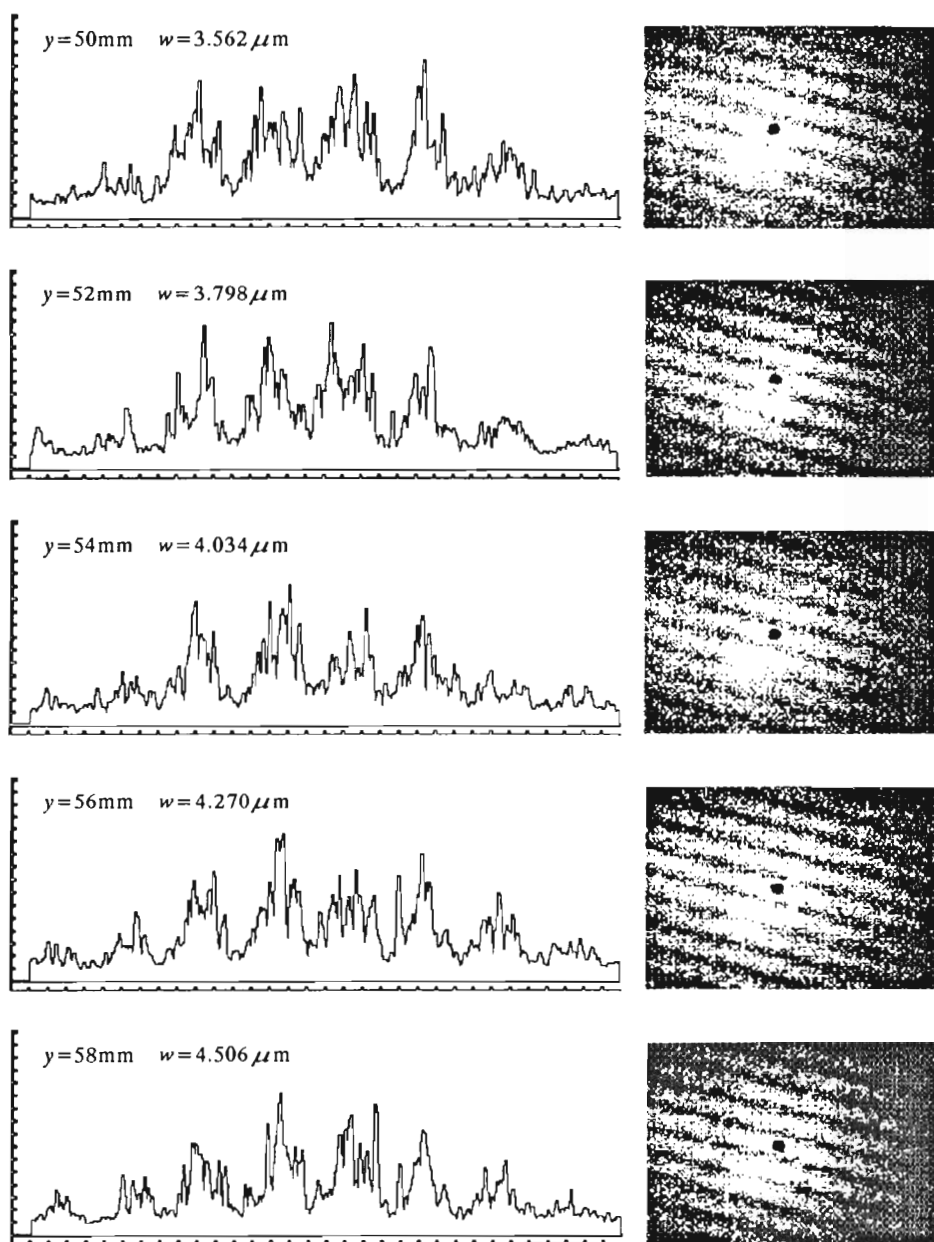


Fig. 4. Determination of small strain in the CoMoNi amorphous alloy. The histogram is calculated in the direction parallel to the tension direction

20 mm from the processor optical axis. For all the analyzed zones of the specklegram, the functions  $J_0(u, v)$  and  $N(u, v)$  differ only in the scale factor, which is proportional to the diffraction yield of the specklegram zone. It enables determination of small strains with the accuracy of  $10^{-6} \div 10^{-7}$ . Algorithms described by Pisarek (1994) has been applied to the analysis of strains. Distortion in the light distribution symmetry due to processor errors, visible in Fig.4, can be eliminated numerically straight forward.

### 5.3. Fourier halos for translation and rotation

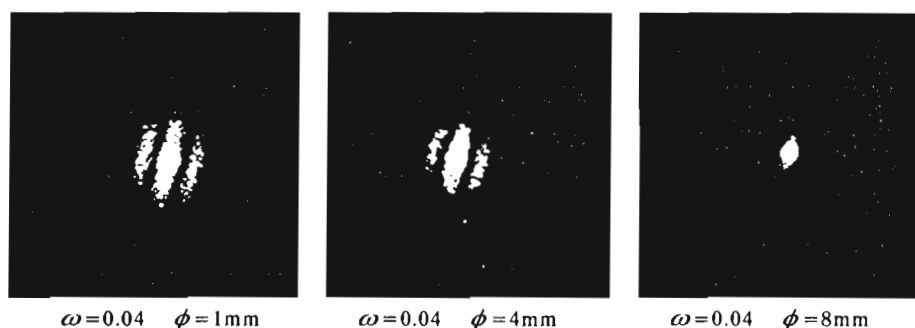


Fig. 5. Fringe spoiling due to a large rotation angle and a big diameter of the analyzed region

If the tensor of relative displacement has only antisymmetrical component then the coefficient  $N(u, v)$  must be a central symmetric function. In Fig.5 and Fig.6 the Fourier halos of the specklegrams which have been registered in white light are presented. The region of contrast fringe, visible in Fig.5, is affected by the rotation angle. The fringe contrast is modulated by the central symmetric function, defined by Eq (3.5). For large rotation angles  $\omega$  and very big diameter  $\phi$  no fringe is visible.

Fig.6 presents different configurations of the rotation angles  $\omega$  and the processor diaphragm diameters  $d$ , respectively. If products of these values are equal, then the corresponding halos have to be (see Eq (3.4) and (3.5)) modulated by the same contrast function  $N(u, v)$ . The diameters of visible fringe regions should be, according to Eq (3.5) determined by the product  $d \otimes \omega$ . Small differences between calculated and experimentally registered images appear due to instability of the photo-chemical image development process.

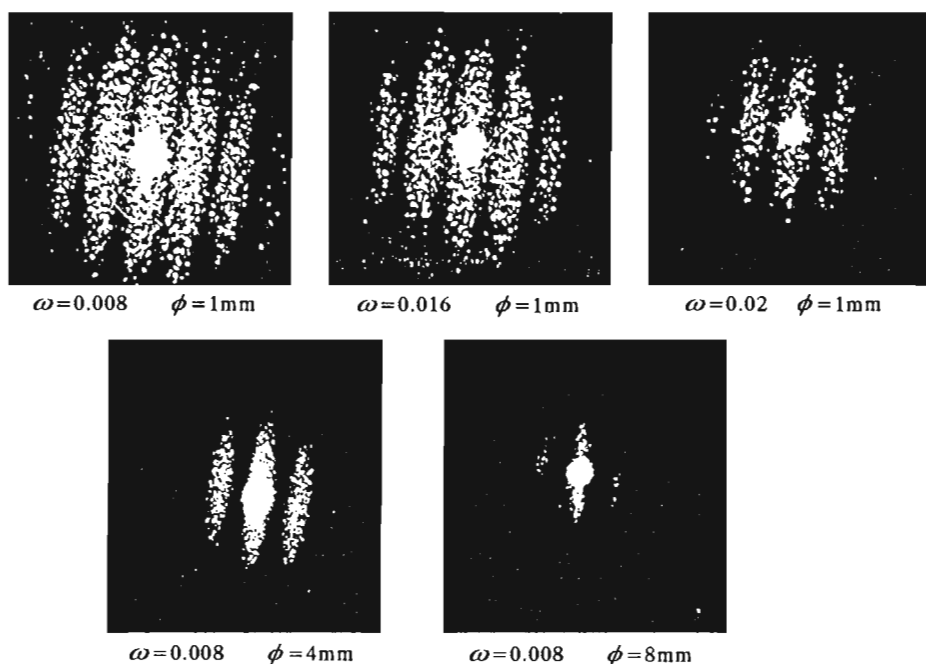


Fig. 6. Contrast and granularity of the Fourier halo for the superposition of translation and rotation

The processor diaphragm diameter determines not only the contrast function but also the image speckling. For small diameter values the great granularity of the Fourier halo image is visible. We have to take this effect (described by the second component in Eq (4.2)) into account when formulating the image analysis algorithm.

#### 5.4. Fourier halos for displacement and great strains

In Fig.7a the Fourier halos of selected regions of the photoelastic model are presented for a plexiglas plate loaded by three-force-system (Fig.7b). The specklegram has been registered in white light. The displacement gradient at the point  $E$  has only strain components  $(\varepsilon_1, \varepsilon_2)$  and the direction of  $\varepsilon_1$  is parallel to the plate edge. Because the processor is supplied with a circle diaphragm zero points of the contrast function calculated from Eq (3.6) are located on the ellipse major axis which is perpendicular to the plate edge. At the points  $A - C$  the displacement gradient has both the strain and rotation

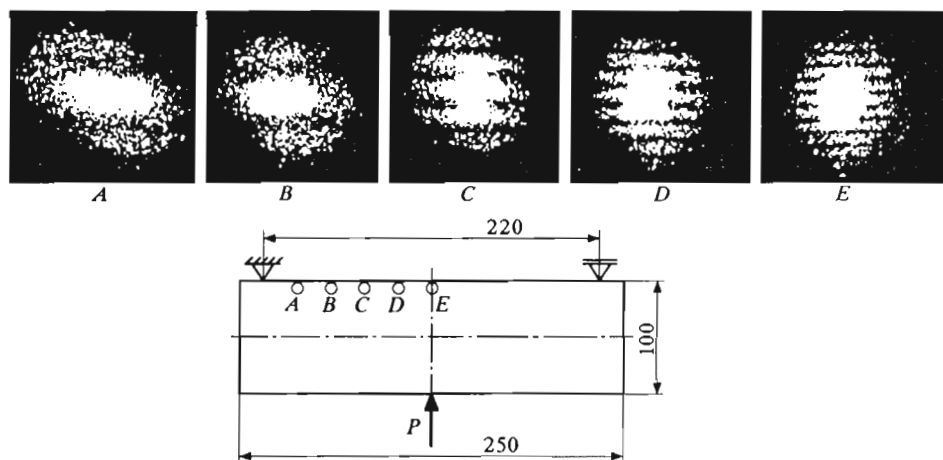


Fig. 7. Typical specklegram halos for the superposition of translation, rotation and strain

components. The rotation affects a change of direction of the calculated contrast function axis of symmetry. The largest rotation angle calculated from Eq (3.5) appears at the point A.

## 6. Conclusions

The speckle photography is a very precise method for the displacement and strain fields measurements. The theory presented enables optimization of the class of approximation functions, used in a numerical analysis of the specklegram Fourier halo. It is important however to eliminate systematic errors of the method.

For small displacement gradients the range and accuracy of displacement determination depends on the basic speckle pattern, which can be quantitatively described by the characteristic function. This function can be affected either by optical parameters of the camera used for the specklegram registration or by the surface roughness of the analyzed object. The concept of characteristic function is useful in quantitative description of speckle pattern made in laser light and in white light too.

For great displacement gradients the accuracy of displacement measurements depends on the diaphragm shape function in the Fourier processor and on the displacement gradient. Contrast of the observed fringe pattern is repre-

sented by the coefficient  $N(u, v)$  defined as the Fourier transform of diaphragm shape function. Scale factors of this transform are linear combinations of the displacement gradient components. The reduction of diaphragm size involves, however, considerable granularity of the specklegram halo, which may result in a substantial increase in random errors.

### References

1. ARCHBOLD E., BURCH J.M., ENNOS A.E., 1970, Recording of in Plane Displacement by Double-Exposure Speckle Photography, *Optica Acta*, **17**, 12, 883-98
2. BACHMACZ W., PISAREK J.P., 1980, Wyznaczanie statycznych i dynamicznych przemieszczeń dużych obiektów metodą interferometrii plamkowej w świetle białym, *Mat. IX Symp. Badań Dośw. w Mechanice Ciała Stałego*
3. BACHMACZ W., PISAREK J.P., 1983, Pomiary przemieszczeń normalnych do powierzchni obiektu metodą fotografii plamkowej w świetle białym, *Mechanika Teoretyczna i Stosowana*, **21**, 1, 79-80
4. BERNABEU E., AMARE J.C., ERROYO M.P., 1985, White Light Speckle Method of Measurement of Flow Velocity Distribution, *Applied Optics*, **21**, 14, 44-52
5. BURCH J.M., TOKARSKI J.M.J., 1968, Production of Multiple Beam Fringes from Photographic Scatterers, *Optic Acta*, **15**, 2, 101
6. CATHEY W.T., 1980, *Optyczne przetwarzanie informacji i holografia*, PWN, Warszawa
7. CHIANG F.P., JUANG R.M., 1976a, Laser Speckle Interferometry for Plate Bending Problems, *Applied Optics*, **15**, 9, 2199-2204
8. CHIANG F.P., JUANG R.M., 1976b, Vibration Analysis of Plate and Shell by Laser Speckle Interferometry, *Optica Acta*, **23**, 12, 997-1009
9. CHIANG F.P., BAILANGALADI M., 1980, White Light Projection Speckle Method for Generating Deflection Contours, *Applied Optics*, **19**, 15, 2623-2626
10. DUDDERAR T.D., MEYNART R., SIMPKINS P.G., 1988, Laser Metrology for Fluid Velocity Measurement, *Optics and Lasers in Engineering*, **9**, 163-199
11. ERF R.K., 1978, *Speckle metrology*, Academic Press, New York
12. FORNO C., 1975, White-Light Speckle Photography for Measuring Deformation, Strain and Shape, *Optics and Laser Technology*, **10**, 217-221
13. FRANCON M., 1980, *La granularité laser (speckle) et ses applications en optique*, Russian transl., *Optica sp'eklov*, J.Ostrowski, Mir, Moskva

14. IWATA K., HAKOSHIMA T., NAGATA R., 1978, Measurement of Flow Velocity Distribution by Multiple Exposure Speckle Photography, *Optics Communications*, **25**, 3, 311-314
15. PARKS V.J., 1980, The Range of Speckle Metrology, *Experimental Mechanics*, **6**, 181-191
16. PISAREK J. T., 1986, Doświadczalna analiza odkształceń i przemieszczeń metodami fotografii plamkowej w świetle białym, Thesis, Politechnika Częstochowska, Częstochowa
17. PISAREK J.T., 1984, O transformacie Fouriera pewnej funkcji stochastycznej, *Ref. 13 konf. Zastosowań Matematyki*, Sielpia, 17-26 IX 1984
18. PISAREK J.T., 1994, Characteristic Function in Description of Speckle Pattern, *Konf. GAMM'94*, Braunschweig
19. PISAREK J.T., 1995, Characteristic Function in Description of Speckle Pattern, *Zeitschrift für Angewandte Mathematic und Mechanik*, **75**, 299-300
20. PISAREK J.T., 1994, Algorithms of Specklegram Analyse, *Procedings SPIE-Interferometry'94-Photomechanics*, **2342**, 155-159

## Pomiar gradientu pola przemieszczeń przy pomocy fotografii plamkowej

### Streszczenie

W pracy opisano ilościowo wpływ tensora przemieszczeń względnych na widmo fourierowskie specklogramu. Wykazano, że rozkład energii w widmie jest zależny od rodzaju struktury plamkowej i współczynnika przemieszczeń względnych, definiowanego jako transformata Fouriera funkcji kształtu analizowanego podobszaru specklogramu. Czynnikiem skalującym przekształcenia są dobrane odpowiednio składowe tensora przemieszczeń względnych. Powyższe wyniki zostały zweryfikowane doświadczalnie dla różnych stanów przemieszczeń, odkształceń i rotacji przy pomocy punktowego procesora Fourierowskiego, sprzężonego z komputerem osobistym.

*Manuscript received June 21, 1995; accepted for print December 4, 1995*